HHS Public Access

Author manuscript

Nat Chem Biol. Author manuscript; available in PMC 2018 October 01.

Published in final edited form as:

Nat Chem Biol. 2017 October ; 13(10): 1102–1108. doi:10.1038/nchembio.2458.

Small-molecule studies identify CDK8 as a regulator of IL-10 in myeloid cells

Liv Johannessen[1,2,13], **Thomas B Sundberg**[3,13], **Daniel J O'Connell**[4], **Raivo Kolde**[5], **James Berstler**[3], **Katelyn J Billings**[6,7], **Bernard Khor**[5], **Brinton Seashore-Ludlow**[7], **Anne Fassl**[2,8], **Caitlin N Russell**[9], **Isabel J Latorre**[4], **Baishan Jiang**[1,2], **Daniel B Graham**[4,10], **Jose R Perez**[3], **Piotr Sicinski**[2,8], **Andrew J Phillips**[3], **Stuart L Schreiber**[7,11,12], **Nathanael S Gray**[1,2,*], **Alykhan F Shamji**[7,*], and **Ramnik J Xavier**[4,5,9,*]

[1]Department of Biological Chemistry and Molecular Pharmacology, Harvard Medical School, Boston, Massachusetts, USA

[2]Department of Cancer Biology, Dana–Farber Cancer Institute, Boston, Massachusetts, USA

[3]Center for the Development of Therapeutics, Broad Institute, Cambridge, Massachusetts, USA

[4]Infectious Disease and Microbiome Program, Broad Institute, Cambridge, Massachusetts, USA

[5]Center for Computational and Integrative Biology, Massachusetts General Hospital, Boston, Massachusetts, USA

[6]Department of Chemistry, Yale University, New Haven, Connecticut, USA

[7]Center for the Science of Therapeutics, Broad Institute, Cambridge, Massachusetts, USA

[8]Department of Genetics, Harvard Medical School, Boston, Massachusetts, USA

[9]Gastrointestinal Unit and Center for the Study of Inflammatory Bowel Disease, Massachusetts General Hospital, Boston, Massachusetts, USA

[*] Nathanael_Gray@DFCI.HARVARD.EDU, ashamji@broadinstitute.org or xavier@molbio.mgh.harvard.edu.

[13]These authors contributed equally to this work.

Competing financial interests

L.J., T.B.S., B.K., J.R.P., N.S.G., A.F.S., and R.J.X. are co-inventors on a provisional patent application based on these results. The authors declare competing financial interests: details accompany the online version of the paper.

Author contributions

L.J. designed studies, conducted experiments, analyzed results and wrote the paper. T.B.S. devised the project, developed the screen, designed studies, conducted experiments, analyzed results and wrote the paper. D.J.O. designed studies, conducted experiments and analyzed results. R.K. analyzed gene expression and multiplex reporter data. J.B. designed studies, conducted experiments and analyzed results. K.J.B. synthesized BRD0330 analogs. B.K. designed studies, conducted experiments and analyzed results. B.S.-L. designed studies, conducted experiments and analyzed results. A.F. generated *Ccnc*$^{\Delta/\Delta}$ mice. C.N.R. conducted the screen. I.J.L. designed studies and analyzed results. B.J. synthesized CCT251921. D.B.G. designed studies, conducted experiments and analyzed results. J.R.P. designed studies, conducted experiments and analyzed results. P.S. generated *Ccnc*$^{\Delta/\Delta}$ mice. A.J.P. designed studies, conducted experiments and analyzed results. S.L.S. designed studies, analyzed results and wrote the paper. N.S.G. designed studies, analyzed results and wrote the paper. A.F.S. devised the project, developed the screen, synthesized CCT251921, designed studies, analyzed results and wrote the paper. R.J.X. devised the project, developed the screen, designed studies, analyzed results and wrote the paper.

Additional information

Any supplementary information, chemical compound information and source data are available in the online version of the paper. Reprints and permissions information is available online at http://www.nature.com/reprints/index.html. Publisher's note: Springer Nature remains neutral with regard to jurisdictional claims in published maps and institutional affiliations. Correspondence and requests for materials should be addressed to N.S.G., A.F.S. or R.J.X.

[10]Department of Medicine, Massachusetts General Hospital, Harvard Medical School, Boston, Massachusetts, USA

[11]Department of Chemistry and Chemical Biology, Harvard University, Cambridge, Massachusetts, USA

[12]Howard Hughes Medical Institute, Cambridge, Massachusetts, USA

Abstract

Enhancing production of the anti-inflammatory cytokine interleukin-10 (IL-10) is a promising strategy to suppress pathogenic inflammation. To identify new mechanisms regulating IL-10 production, we conducted a phenotypic screen for small molecules that enhance IL-10 secretion from activated dendritic cells. Mechanism-of-action studies using a prioritized hit from the screen, BRD6989, identified the Mediator-associated kinase CDK8, and its paralog CDK19, as negative regulators of IL-10 production during innate immune activation. The ability of BRD6989 to upregulate IL-10 is recapitulated by multiple, structurally differentiated CDK8 and CDK19 inhibitors and requires an intact cyclin C–CDK8 complex. Using a highly parallel pathway reporter assay, we identified a role for enhanced AP-1 activity in IL-10 potentiation following CDK8 and CDK19 inhibition, an effect associated with reduced phosphorylation of a negative regulatory site on c-Jun. These findings identify a function for CDK8 and CDK19 in regulating innate immune activation and suggest that these kinases may warrant consideration as therapeutic targets for inflammatory disorders.

The anti-inflammatory cytokine IL-10 promotes immune homeostasis via multiple mechanisms including suppressing inflammatory cytokine production by innate immune cells and by promoting regulatory T cell (T_{reg}) function[1]. Genetic studies of inflammatory bowel disease (IBD) have linked single-nucleotide polymorphisms near *IL10* to adult-onset IBD and identified rare, loss-of-function mutations in *IL10* or its receptor that result in severe, pediatric-onset enterocolitis[2]. Conversely, IL-10-based therapy reduces disease activity in murine models of colitis, bacterial infection, psoriasis and arthritis[3]. In addition, oral administration of bacteria engineered to express IL-10 and injection of a fusion protein in which recombinant IL-10 (rIL-10) is coupled to an inflammation-targeting antibody have shown promise in clinical trials for Crohn's disease and rheumatoid arthritis, respectively[4,5]. Hence, while impaired function of IL-10 or its receptor can lead to inflammation, augmenting IL-10 abundance or signaling may be viable therapeutic strategies to restore and maintain immune homeostasis.

Small-molecule probes have provided key insights into regulation of IL-10 in innate immune cells. Activators of cAMP-response element binding protein (CREB)-dependent transcription such as G-protein-coupled receptor agonists or inhibitors of phosphodiesterases (PDEs), salt-inducible kinases (SIKs), or glycogen synthase kinase-3β (GSK-3β) potentiate IL-10 production in macrophages and dendritic cells[6–9]. Alternatively, amplification of mitogen-activated-protein (MAP) kinase signaling by perturbation of microtubule dynamics or inhibition of cyclin-dependent kinase 5 (CDK5) can also upregulate IL-10 (refs. [10,11]). Notably, these probes have identified therapeutically useful drug targets, exemplified by

approval of the PDE4 inhibitor apremilast for treatment of psoriatic arthritis as well as preclinical evaluation for treatment of IBD[12,13].

Based on these successes, we conducted an unbiased phenotypic screen for small-molecule enhancers of IL-10 production with the goal of identifying new mechanisms of IL-10 regulation and, potentially, new targets for development of anti-inflammatory therapies. Subsequent mechanism-of-action (MoA) studies identified the transcriptional regulatory kinase CDK8 and its paralog CDK19 as molecular targets for the prioritized screening hit BRD6989 (**1**). Along with BRD6989, multiple structurally differentiated CDK8 and CDK19 inhibitors also upregulated IL-10 in activated human and mouse dendritic cells, and this effect required an intact cyclin C–CDK8 complex. Finally, using a multiplexed pathway reporter assay, we identified a role for enhanced activator protein 1 (AP-1) transcriptional activity in IL-10 potentiation following inhibition of CDK8 and CDK19, and demonstrated that this effect is associated with reduced phosphorylation of a negative regulatory site on c-Jun. Together, these findings suggest that inhibitory phosphorylation of c-Jun by CDK8 is a previously uncharacterized mechanism regulating IL-10 production during innate immune activation.

RESULTS

Identification of small molecules that upregulate IL-10

To identify new mechanisms of IL-10 regulation, we screened 59,346 small molecules for the ability to enhance IL-10 production by activated bone-marrow-derived dendritic cells (BMDCs) using a high-throughput assay that we developed previously[9]. Compounds were derived from both commercial collections and structurally and skeletally diverse libraries prepared by diversity-oriented synthesis (DOS). We identified >60 hit compounds that reproducibly enhance IL-10 production in a concentration-dependent manner (Supplementary Results, Supplementary Table 1). We prioritized three distinct chemotypes for follow-up studies on the basis of potency and an initial analysis of structure–activity relationship (SAR) with respect to core scaffold, stereochemistry and side chains (Fig. 1a). Among these, the DOS-derived hits BRD10330 (**2**) and BRD70326 (**3**) were deprioritized on the basis of data showing that they stimulated production of the inflammatory cytokine IL-1β and suppressed microtubule polymerization, respectively (Supplementary Figs. 1 and 2).

Prioritized hit BRD6989 selectively upregulates IL-10

The pyridinyl tetrahydroquinoline BRD6989 emerged as a prioritized hit in our screen (Fig. 1a and Supplementary Table 2). Pretreatment of BMDCs with BRD6989 for 48 h followed by stimulation with the yeast cell wall extract zymosan A for 18 h increased IL-10 production with an effector concentration for half-maximum response (EC_{50}) ~1 μM (Fig. 1b), while only modestly reducing cell viability in these assay conditions (Supplementary Fig. 3). In addition, BRD6989 suppressed zymosan A–induced release of the inflammatory cytokine IL-6, but left production of TNFα, IL-12p40 and IL-1β largely unchanged (Fig. 1c and Supplementary Fig. 3). BRD6989 induced similar cytokine responses in BMDCs stimulated with the viral RNA mimetic R848 but with a greater fold-increase in IL-10

production (Fig. 1d and Supplementary Fig. 3). In addition to BMDCs, BRD6989 increased IL-10 production in mouse bone-marrow-derived macrophages (BMDMs) activated with zymosan A or R848 (Supplementary Fig. 3). Lastly, BRD6989 upregulated IL-10 following R848 stimulation in human, monocyte-derived DCs from two independent donors at concentrations consistent with its activity in BMDCs (Fig. 1d and Supplementary Fig. 3). Thus, BRD6989 enhances IL-10 production in activated human and murine macrophages and dendritic cells by a mechanism that appears to be particularly pronounced following stimulation of toll-like receptor-7 (TLR7) and TLR8 by R848.

Analyzing the effects of BRD6989 pretreatment on *Il10* mRNA levels after R848 stimulation revealed a sustained increase beginning at 4 h and extending to 24 h (Supplementary Fig. 3). These *Il10* transcript dynamics contrast with activators of CREB-dependent transcription such as the pan-SIK (salt-inducible kinase) inhibitor HG-9-91-01 (**4**)[8], which elevated *Il10* mRNA during the first 2 h following microbial stimulation before returning to levels similar to DMSO-treated cells (Supplementary Fig. 3). Based on its ability to selectively potentiate IL-10 production by a mechanism that appears temporally distinct from CREB activation, we prioritized BRD6989 for MoA studies.

Mediator-associated kinase CDK8 is a target of BRD6989

Given that the pyridine core of BRD6989 is a common kinase-binding motif[14], we profiled its effects on 414 kinases using a combination of binding and activity assays. We found that BRD6989 binds a complex of cyclin C–CDK8, a Mediator-associated kinase not previously linked to IL-10 regulation[15], with a half-maximal inhibitory concentration (IC_{50}) ~200 nM and remarkable selectivity (Fig. 2a and Supplementary Fig. 4 and Supplementary Data Set 1). Binding of BRD6989 to CDK8 and its paralog CDK19 was confirmed using an orthogonal kinase-profiling format (Supplementary Data Set 2). In addition to CDK8, both kinase profiling experiments identified phosphatidylinositol-4,5-biphosphate 3-kinase C2A (PI3KC2A) and PI3KCG as secondary targets of BRD6989, suggesting an overall consistency between these approaches. Of note, PI3K inhibitors with varying isoform specificities screened in our assay system fail to enhance IL-10 production[9], suggesting that inhibition of PI3Ks does not contribute to IL-10 potentiation by BRD6989.

In agreement with the kinase profiling results, BRD6989 inhibits the kinase activity of recombinant cyclin C–CDK8 or cyclin C–CDK19 complexes with IC_{50}s ~0.5 μM and >30 μM, respectively (Fig. 2b), but not the activity of several CDKs involved in cell cycle regulation (Supplementary Fig. 4). Furthermore, pre-incubation of BMDCs with BRD6989 inhibited IFNγ-induced phosphorylation of signal transducer and activator of transcription 1 (STAT1) at the known CDK8-regulated position Ser727 (ref. 16), but did not affect Janus kinase (JAK)-mediated phosphorylation of Tyr701 (Fig. 2c). Preliminary SAR analysis of BRD6989's effects on CDK8 and IL-10 suggest that the pyridine and amino substituents and the methyl cyclohexyl core of BRD6989 make critical contacts with CDK8 (Supplementary Fig. 5). Notably, the potency of CDK8 binding correlates with that of IL-10 induction for these analogs (Fig. 2d), whereas BRD6989 only inhibits CDK19 at concentrations much greater than the EC_{50} for IL-10 induction. Together, these kinase profiling, binding assay,

enzyme inhibition and cell-based data identify the Mediator-associated kinases CDK8 and, to a lesser degree, CDK19 as molecular targets of BRD6989.

Structurally distinct CDK8 inhibitors upregulate IL-10

Burgeoning interest in Mediator-associated kinases as chemotherapeutic targets has prompted development of several structurally distinct CDK8 and CDK19 inhibitors including Δ^{16}-cortistatin A (dCA; **5**), an analog of the potent CDK8- and CDK19-selective natural product cortistatin A[17,18], and the recently published highly selective CDK8 and CDK19 inhibitor CCT251921 (**6**)[19] (Fig. 3a). Pretreatment with these CDK8 and CDK19 inhibitors recapitulated the IL-10 potentiating activity of BRD6989 in both BMDCs (Fig. 3b) and human DCs derived from two independent donors with R848 stimulation (Fig. 3c and Supplementary Fig. 6). Notably, the IL-10 potentiating activity of these three inhibitors occurs at concentrations consistent with their potencies for CDK8 and CDK19 inhibition. By contrast, IL-10 production is not enhanced by the CDK7-targeting inhibitor THZ-1 (ref. 20) (**7**) (Supplementary Fig. 6), suggesting that this effect is not a nonspecific consequence of inhibiting transcriptional regulatory kinases. Lastly, the effect of CDK8 inhibition on IL-10 production may be cell-type-specific, because neither dCA nor BRD6989 dramatically increased IL-10 production during *ex vivo* differentiation of T_{reg}s (Supplementary Fig. 6). Together, these data support CDK8 inhibition as the mechanism driving IL-10 potentiation in response to BRD6989 in activated human and murine DCs.

IL-10 elevation requires intact cyclin C–CDK8 complexes

Next, to determine whether IL-10 potentiation by CDK8 inhibitors requires functional cyclin C–CDK8 complexes, we differentiated between BMDCs from *Ccnc*$^{\Delta/\Delta}$ mice[21], in which the floxed *Ccnc*$^{fl/fl}$ allele had been specifically disrupted in hematopoietic cells by induction of *Mx1-Cre* following stimulation with polyinosinic–polycytidylic acid (poly(I:C)) (Supplementary Fig. 7). As a control, BMDCs were differentiated from poly(I:C)-treated littermates expressing the *Ccnc*$^{fl/fl}$ allele, but lacking *Mx1-Cre*. Notably, there was not a statistically significant difference in the levels of IL-10 secreted between *Ccnc*$^{\Delta/\Delta}$ and *Ccnc*$^{f/f}$ following R848 stimulation (Supplementary Fig. 7), suggesting that other regulatory mechanisms can compensate for a sustained loss of CDK8 activity and maintain low basal levels of IL-10 production. However, *Ccnc*$^{\Delta/\Delta}$ BMDCs failed to upregulate IL-10 in response to treatment with dCA or BRD6989, whereas the response remained intact in *Ccnc*$^{f/f}$ BMDCs (Fig. 3d,e and Supplementary Fig. 7). In addition, *Ccnc*$^{\Delta/\Delta}$ BMDCs displayed a ~50% reduction in IL-6 production relative to *Ccnc*$^{f/f}$ BMDCs, and saturating concentrations of dCA or BRD6989 caused no further reduction (Fig. 3d,e). Cyclin C deletion does not appear to inhibit cytokine production nonspecifically, as it does not affect IL-10 and IL-6 responses induced by the pan-SIK inhibitor HG-9-91-01 (Supplementary Fig. 7). The impaired responses of BMDCs lacking cyclin C to treatment with BRD6989 and dCA are consistent with a model in which CDK8 restrains IL-10 production during activation of wild-type myeloid cells.

CDK8 represses a small subset of genes in macrophages

To define systematically the role of CDK8 during innate immune activation, we profiled the transcriptional responses elicited by dCA or BRD6989 following stimulation of BMDMs with a panel of ten microbial ligands or Sendai virus for time points from 0.25 to 4 h. BMDMs were chosen for these experiments because, like human and mouse DCs, they upregulate IL-10 in response to CDK8 inhibition (Supplementary Fig. 3), and they have been previously studied using the multiplexed pathway reporter assay described below[22]. In this experiment, the transcriptional responses elicited by BRD6989 and dCA were highly correlated (Supplementary Fig. 8), again supporting CDK8 as a principle cellular target of BRD6989. For instance, both of the CDK8 inhibitors reduced expression of the interferon-inducible genes *Ifit2*, *Cxcl10* and *Rsad2* (Supplementary Fig. 8). Given that CDK8-dependent phosphorylation of STAT1 at S727 is required for expression of many IFNγ-inducible genes[16], these suppressive effects suggest that CDK8 inhibition may limit autocrine interferon signaling following microbial stimulation.

In addition to suppressing interferon-inducible genes, BRD6989 and dCA increased abundance of a similar, small subset of transcripts in both quiescent and activated BMDMs (Supplementary Fig. 8). Consistent with the effects of CDK8 inhibition on cytokine responses in activated myeloid cells, the genes induced include chemokines, metallopeptidases and regulators of cellular second messengers linked to inflammatory responses and migration of innate immune cells ($P = 0.0255$ and $P = 1.52 \times 10^{-5}$, respectively) (Supplementary Data Set 3). In the context of acute myeloid leukemia (AML), CDK8 inhibition preferentially induces genes near ‘super enhancers’ (SEs), defined by dense binding of the Mediator complex and transcription factors along with accumulation of histone modifications associated with active transcription[18]. Acknowledging the limitations in comparing data sets from different myeloid cell types, we queried genes upregulated in BRD6989- or dCA-treated BMDMs for the presence of histone modifications linked to active transcription that were previously identified in lipopolysaccharide (LPS)-stimulated BMDCs[23]. In this analysis, monomethylated Lys-4 on histone 3 (H3K4me1), a mark associated with poised enhancers[24,25], is enriched ($P = 0.0093$) near genes induced by CDK8 inhibition compared to all highly expressed genes (Supplementary Fig. 8). Although we detect a similar trend in regard to enrichment of histone 3 Lys27 acetylation (H3K27ac), a modification associated with active enhancers[24,25], near genes that are induced by CDK8 inhibition, this association did not achieve statistical significance (Supplementary Fig. 8). These data indicate that CDK8 primarily represses a small set of genes in quiescent or activated macrophages, although the link between CDK8-regulated genes and histone modifications associated with active transcription appears to be less well correlated in this context.

Enhanced AP-1 activity links CDK8 inhibition to IL-10

To identify CDK8-responsive signaling pathways, we applied an integrative genomics approach termed transcription factor sequencing (TF-seq) in which consensus transcription factor binding sites drive expression of 58 reporter constructs bearing unique sequence tags[22]. Consistent with the established role of CDK8 in STAT1 activation[16], BRD6989 and dCA both suppressed induction of STAT1–STAT2 activity ~2 h after stimulation of BMDMs

(Fig. 4a; Supplementary Fig. 9 and Supplementary Data Set 4). Furthermore, similar to results from previous studies of CDK8 function in other contexts including RPMI8226 myeloma cells activated by TLR9 stimulation[26–28], pretreatment with dCA or BRD6989 suppressed NF-κB activation to a varying degree for all stimuli tested (Fig. 4a and Supplementary Fig. 9). Because dCA pretreatment does not perturb upstream signaling events that link sensing of LPS or R848 to NF-κB activation (Supplementary Fig. 9), it appears that inhibiting CDK8 may suppress the ability of nuclear NF-κB to activate transcription.

TF-seq results also indicate that CDK8 inhibition increases AP-1 activity in BMDMs (Fig. 4a and Supplementary Fig. 10). In support of this observation, binding sites for the AP-1 subunit JunB are enriched among genes upregulated following CDK8 inhibition compared to to all highly expressed genes (Fig. 4b). Given that c-Jun's ability to activate transcription is tightly regulated by phosphorylation, we tested whether CDK8 inhibition affects c-Jun phosphorylation in activated BMDCs. We found that pretreatment with dCA only moderately delayed the activating phosphorylation of c-Jun on Ser63, an effect that is rapidly induced by R848 stimulation and peaks after 30 min (Fig. 4c). In contrast, inhibiting CDK8 with dCA dramatically reduced phosphorylation of Ser243, a suppressive mark shown to destabilize c-Jun and interfere with its ability to bind DNA[29–31], which is first observed 60 min after R848 stimulation (Fig. 4c). Notably, dCA induces concentration-dependent suppression of c-Jun Ser243 phosphorylation both in R848-stimulated BMDCs (Supplementary Fig. 10) and an *in vitro* kinase reaction with recombinant cyclin C–CDK8 and c-Jun (Fig. 4d). Together, these data suggest that c-Jun Ser243 is a direct CDK8 substrate that regulates AP-1 activity in activated myeloid cells.

Given the presence of an AP-1 consensus motif in *Il10* and the evidence that potentiation of MAP kinase signaling can increase IL-10 production[1,10,11], we hypothesized that an increase in AP-1 activity resulting from reduced c-Jun Ser243 phosphorylation may mediate activation of IL-10 following CDK8 inhibition. Supporting this theory, we found that co-treatment of BMDCs with dCA and T-5224 (8), a small-molecule inhibitor of AP-1 reported to bind c-Fos and inhibit its dimerization with c-Jun[32] (Supplementary Fig. 10), suppressed IL-10 production following stimulation with R848 or zymosan A (Fig. 4e,f). Although the concentration of T-5224 (100 μM) that suppressed IL-10 potentiation by dCA is consistent with concentrations needed to prevent c-Jun binding to AP-1 elements[32], it is possible that the decrease in IL-10 induction could be due to nonspecific effects of T-5224 on myeloid cell function. However, the same concentration of T-5224 did not: 1) Affect the ability of BMDCs to increase in IL-10 production in response to potentiation of CREB signaling by the pan-SIK inhibitor HG-9-91-01; or, 2) Suppress production of IL-6 or TNFα by R848-stimulated BMDCs (Supplementary Fig. 10). These data suggest that T-5224 does not nonspecifically impair the ability of BMDCs to respond to microbial stimulation. Together with the increase in AP-1 transcriptional activity and reduced c-Jun Ser243 phosphorylation, the inhibitory effect of T-5224 suggests that CDK8 inhibition upregulates IL-10 production by a c-Jun–AP-1-dependent mechanism that is distinct from cAMP and CREB signaling.

DISCUSSION

Using unbiased phenotypic screening and MoA studies, we have identified the Mediator-associated kinase CDK8 and, likely, its paralog CDK19 as regulators of IL-10 production, a mechanism that may be harnessed to enhance anti-inflammatory functions of innate immune cells. Our initial screen uncovered three new structural classes of small molecules that enhance IL-10 production including BRD6989, a probe found to bind to CDK8 through kinase profiling. The growing interest in Mediator-associated kinases as therapeutic targets in cancer has spurred development of several chemically distinct CDK8 and CDK19 inhibitors such as the potent, dual inhibitor CCT251921 (ref. 19), which shares a pyridinyl tetrahydroquinoline core with BRD6989, and a close analog of the natural product cortistatin A (dCA)[17,27]. Though not as potent as these inhibitors, BRD6989 appears to be unique in its ability to differentially inhibit CDK8 relative to its paralog CDK19, suggesting that it may inform further development of CDK8-specific inhibitors. Importantly, we found that both CCT251921 and dCA, similarly to BRD6989, promote IL-10 production in R848-stimulated human and mouse DCs in a manner that depends on an intact cyclin C–CDK8 complex. Together, these data identify CDK8 as a druggable regulator of IL-10 production in activated myeloid cells.

In comparison to CDK7 and CDK9, which broadly affect transcriptional initiation by activating phosphorylation of the C-terminal domain of RNA polymerase II[20,33], CDK8's function appears to be more context dependent, having been linked to specific effects on interferon, TGF-β, Wnt and Notch signaling[15]. For example, phosphorylation of the transactivation domain of STAT1 by CDK8 is required for expression of many interferon-inducible genes[16], and cortistatin A specifically elevates expression of SE-associated genes in a subset of AML lines[18]. Similarly, our transcriptional profiling data in BRD6989- or dCA-treated BMDMs suggest that CDK8's kinase function primarily restrains expression of a limited number of genes in myeloid cells. In contrast to the AML context, our preliminary analysis suggests that genes regulated by CDK8 in myeloid cells are not correlated with regions of active transcription (i.e., SE-associated regions). However, it will be interesting to define experimentally how inhibiting CDK8 activity alters chromatin organization (for example, H3K27ac localization) in myeloid cells.

Measuring the response to CDK8 inhibition using a multiplex pathway reporter assay (TF-seq) provided insights into CDK8-sensitive signaling pathways in activated myeloid cells. Consistent with previous studies implicating CDK8 in IFNγ signaling[16], we observed that inhibition of CDK8 reduced activation of STAT1–STAT2 and triggered a corresponding decrease in expression of several interferon-inducible genes. We also detected decreased NF-κB activity to varying degrees using different microbial stimuli that appears to be insufficient in magnitude to suppress expression of NF-κB targets on a genome-wide scale. This intermediate suppressive effect may explain why CDK8 inhibition does not block expression of *Il10*, itself an NF-κB target gene[28,34]. Our data with dCA and BRD6989 contrasts with the recent identification of an essential role for CDK8 and CDK19 in NF-κB-dependent *Il10* expression following stimulation of TLR9 in the B cell–derived myeloma cell line RPMI8226 (ref. 28). Whereas differences in cell type and microbial stimuli may alter the degree to which NF-κB activation depends on CDK8 and CDK19, contrasting

effects of depleting CDK8 and CDK19 by RNA interference compared to specifically inhibiting their kinase activity with small molecules may also play a role.

CDK8 inhibition also increased AP-1 reporter activity in the TF-seq assay for nearly all microbial stimuli tested, and binding sites for the AP-1 subunit JunB are enriched near genes upregulated in response to CDK8 inhibition. Enhanced AP-1 activity appears to be important for potentiation of IL-10 following CDK8 inhibition, as the c-Fos-targeting inhibitor T-5224 suppresses this response. In contrast, disrupting AP-1 activity does not impair the ability of BMDCs to increase IL-10 production through a parallel, CREB-dependent pathway triggered by the pan-SIK inhibitor HG-9-91-01. Reduced phosphorylation of the negative regulatory site Ser243 on c-Jun may be central to the mechanism linking CDK8 inhibition to enhanced AP-1 transcriptional activity and IL-10 production in myeloid cells. Importantly, CDK8 appears to directly phosphorylate Ser243 in a cell-free biochemical assay and is inhibited by concentrations of dCA that stimulate IL-10 production in cells. Our data identifying CDK8 as a negative regulator of c-Jun–AP-1 in activated myeloid cells contrasts with the role of CDK8 in promoting AP-1 activity during serum stimulation of prostate cancer cells[35]. As such, although CDK8 appears to regulate c-Jun Ser243 phosphorylation following microbial stimulation of postmitotic BMDCs, other kinases targeting this site (for example, casein kinase-2 and Dyrk2a[29,31]) may play this role in cycling cancer cells.

Our data identify the CDK8–c-Jun module as a regulator of IL-10 production that is distinct from previously described pathways such as cAMP–CREB signaling. It remains to be determined whether using CDK8 inhibitors to upregulate IL-10 will be an efficacious and tolerated treatment for inflammatory disorders. The clinical observations that targeted delivery of IL-10 to inflamed tissues can suppress inflammation suggest that recapitulating this strategy with small molecules may hold promise[4,5]. Notably, CDK8 selectively upregulates IL-10 production by activated myeloid cells, suggesting its immunomodulatory activity could be localized to sites of inflammation, circumventing dose-limiting toxicities associated with systemic delivery of IL-10 (refs. [36,37]). In addition, given that increased IL-10 expression and other mechanisms that suppress antitumor immune responses have well-established links to tumor progression and resistance to chemotherapy[38–40], the anti-inflammatory effects of CDK8 and CDK19 inhibition described here warrant consideration in the context of targeting these kinases in cancer.

Given that CDK8 and CDK19 are fundamental regulators of transcription in numerous cell types, it is perhaps not surprising that small-molecule inhibitors of these Mediator-associated kinases are poorly tolerated *in vivo* at doses that achieve the sustained target occupancy required for antitumor activity[41]. Although these toxicities may preclude therapeutic targeting of CDK8 and CDK19, it is possible that the anti-inflammatory consequences of CDK8 and CDK19 inhibition can be achieved *in vivo* using less aggressive dosing regimens. Our data suggest that inhibition of CDK8 and CDK19 affects a limited number of pathways in myeloid cells including several targeted by clinically approved inhibitors of Janus kinases and the proteasome, respectively[42,43]. Thorough investigation of potential toxicities associated with immunomodulatory doses of CDK8 and CDK19 inhibitors *in vivo* will be a

critical next step for evaluating the potential of developing therapeutics targeting these Mediator-associated kinases for treatment of inflammatory disorders.

METHODS

Methods, including statements of data availability and any associated accession codes and references, are available in the online version of the paper.

ONLINE METHODS

Reagents

Unless otherwise indicated, compounds were obtained from the Broad Institute Compound Management Group including (6*R*,7*R*,8*S*)-7-(4-bromophenyl)-8-(hydroxymethyl)-1,4-diazabicyclo[4.2.0]octan-2-one (**21**), a core scaffold used to prepare analogs of BRD10330 (Supplementary Note). Prostaglandin E2 (PGE2) and zymosan A from *Saccharomyces cerevisiae* were purchased from Sigma. BRD6989 (**1**; cat# STL241555) was purchased from Vitas M-Laboratory. BRD8408 (**16**; cat# 75329634) was purchased from ChemBridge. BRD4064 (**17**; cat# F9994-0073) and BRD9548 (**20**; cat# F9994-0072) were purchased from Life Chemicals. BRD5817 (**18**; cat# 6233-1031) and BRD2299 (**19**; cat# 6233-0271) were purchased from ChemDiv. Ultrapure lipopolysaccharide (LPS) from *Escherichia coli* O111:B4. R848, flagellin A (FLA), muramyl dipeptide (MDP), synthetic triacylated lipoprotein (Pam3cys), polyinosinic–polycytidylic acid (Poly(I:C)), and trehalose-6,6-dibehenate (TDB) were purchased from InvivoGen. Sendai virus (Cantell) was purchased from ATCC. Recombinant murine IFNγ, GM-CSF and IL-4 were obtained from Peprotech. T-5224 was obtained from ApexBio. HG-9-91-01 and CCT251921 were prepared as described previously[8,19]. Δ^{16}-cortistatin A (dCA) was a generous gift from P. Baran (The Scripps Research Institute). Small-molecule reagents were confirmed to have ≥95% purity by HPLC–MS.

Isolation and culture of murine macrophages and dendritic cells

Bone marrow was flushed from femurs and tibias of C57BL/6 mice, and preparation of bone-marrow-derived macrophages (BMDMs) and dendritic cells (BMDCs) was conducted as described previously[44]. Unless otherwise indicated, cells were treated for 24 h with BRD6989 (5 μM), dCA (0.1 μM), HG-9-91-01 (0.5 μM) or an equivalent concentration of DMSO (≤0.5%) and then stimulated for 18 h with R848 (2 μg/mL), LPS (100 ng/mL) or zymosan A (4 μg/mL).

Isolation and culture of human dendritic cells (DCs)

For culture of human DCs, $CD14^+$ peripheral blood monocytes (PBMCs) were first enriched from buffy coats obtained from healthy volunteers (Research Blood Components) using RosetteSep Human Monocyte Enrichment Cocktail (cat# 15068) and SepMate 50 centrifugation tube (cat# 85450) according to the manufacturer's protocol (StemCell Technologies). Isolated PBMCs were differentiated into DCs by culturing in X-VIVO10 (Lonza; cat #04-380Q) + FBS (10% v/v) and penicillin–streptomycin (1% v/v) along with GM-CSF (50 ng/mL; Peprotech; cat #300-03) and IL-4 (50 ng/mL; Peprotech; cat #200-04)

for 7 d with additional media and growth factors added on day 4. On day 7, DCs were collected by scraping and plated in 96-well tissue culture plates at 30,000 cells/well before treatment with indicated concentrations of BRD6989, dCA or CCT251921 and an equivalent concentration of DMSO (≤0.5%), and then stimulated for 18 h with R848 (2 μg/mL). After stimulation, tissue culture media was collected and stored at –80 °C before cytokine detection.

High-throughput detection of IL-10 release and cell viability

High-throughput detection of viability and IL-10 release by zymosan A–stimulated BMDCs was conducted as described previously[9].

Connectivity mapping of transcriptional profiling data

Changes in gene expression elicited by BRD0326 (**7**) in U-2 OS osteosarcoma cells have been previously characterized by the Luminex 1000 (L1000) assay[45]. The correlation between the transcriptional responses elicited by BRD0326 and microtubule modulators was identified by comparison with a library of $>1.5 \times 10^6$ gene expression signatures using Broad Institute connectivity mapping database (https://www.broadinstitute.org/cmap/) as described previously[46].

Tubulin polymerization assays

The effect of BRD0326 and related analogs on tubulin dynamics was determined using a fluorescence-based tubulin polymerization assay (Cytoskeleton) according to the manufacturer's protocol.

Kinase profiling

BRD6989 (1 μM) was tested for the ability to bind or inhibit the activity of 414 kinases using either LanthaScreen Eu binding, Adapta or Z-LYTE assays (Invitrogen). Results are presented as percent displacement of dye-labeled probe from the protein kinase domain or remaining kinase activity relative to DMSO (≤0.5%) control (Supplementary Data Set 1). Alternatively, interaction of BRD6989 (10 μM) with a panel of 395 unique kinases was evaluated using the KINOMEscan active site–directed competitive binding assay (DiscoverX). Data are presented as percent displacement of a catalytic-site-directed probe relative to DMSO (≤0.5%) control (Supplementary Data Set 2).

Cyclic C–CDK8 binding assays

Binding of BRD6989 and related analogs to the human cyclin C–CDK8 complex was determined using a LanthaScreen binding assays (Life Technologies) and expressed as percent displacement of a dye-labeled probe from the CDK8 protein kinase domain.

CDK8 and CDK19 kinase activity assays

Effects of BRD6989 on CDK8 or CDK19 activity were quantified using a radiometric filter-binding assay (ProQinase). Briefly, purified recombinant cyclin C–CDK8 or cyclin C–CDK19 were incubated with the indicated dilution series of BRD6989 and changes in

activity quantified in terms of ATP[γ-^{32}P] transfer to the recombinant RBER-IRStide substrate using a radiometric filter binding assay relative to a DMSO (1%) control.

Generation of *Cncc*$^{\Delta/\Delta}$ mice

Male *Ccnc*$^{f/f}$ and *Cncc*$^{\Delta/\Delta}$ (*Ccnc*$^{f/f}$ × Mx1-Cre) mice were generated as described previously using a protocol approved by the Dana–Farber Cancer Institute Animal Care and Use Committee[21]. Briefly, 6–8 week old *Ccnc*$^{f/f}$ and *Cncc*$^{\Delta/\Delta}$ mice were injected with poly(I:C) (2.5 μg g^{-1} intraperitoneally) every other day for 3 d. Femurs and tibias were then harvested from mice sacrificed by CO_2 inhalation overdose followed by cervical dislocation 10 d after the final injection. Recombination of the *Cncc* locus in genomic DNA from BMDCs derived from *Cncc*$^{\Delta/\Delta}$ mice was confirmed using primers P1: 5°-GGGGTGATGGTGAAAACACTGA-3°; P2: 5°-CAAGCAAGTAATCCAGGACCA-3° and P3: 5°-CTGCACATACTGGAGCAAAGGTCT-3° and the following PCR protocol: 95 °C for 3 min, followed by 30 cycles of 95 °C for 1 min, 60 °C for 1 min, 72 °C for 1 min and a final elongation step at 72 C for 5 min.

CDK8–c-Jun kinase reaction

In vitro kinase reactions were carried out for 30 min at 30 °C in assay buffer (60 mM HEPES pH 7.5, 3 mM $MgCl_2$, 3 mM $MnCl_2$, 1.2 mM DTT) using 60 ng recombinant cyclin C–CDK8 (ProQinase; cat# 0376-0390-1), 60 ng recombinant human c-Jun (Abcam; cat# 54318), and 20 μM ATP. CDK8 and c-Jun were pre-incubated with the indicated dilution series of dCA for 15 min before addition of ATP. Reactions were quenched with 10 μL of 80 mM EDTA. To detect c-Jun, 15 μL of the quenched kinase reactions were separated by SDS–PAGE and visualized using the immunoblotting procedure described below.

Immunoblotting

Cell lysis and immunoblotting were conducted as described previously[9]. Briefly, single cell suspensions were rinsed in ice-cold PBS and extracted in lysis buffer (50 mM Tris–HCl at pH 7.4, 1 mM EDTA, 50 mM NaF, 10 mM sodium β-glycerol 1-phosphate, 1 mM DTT, 1 mM sodium orthovanadate, 1% (v/v) Triton X-100, 0.2% (w/v) SDS and 1× Complete EDTA-free Protease Inhibitor Mixture (Roche)). Cell extracts were clarified by centrifugation at 14,000 × *g* for 10 min at 4 °C, and protein concentrations were determined using the Bradford assay (Bio-Rad). To detect proteins in cell lysates, 10–20 μg of protein extract was separated by SDS–PAGE. After transfer to PVDF membranes, proteins were detected by immunoblotting and visualized by treating the blots with SuperSignal West Femto Chemiluminescent Substrate (Thermo Fisher Scientific) followed by autoradiography. The following antibodies were used for immunoblotting: β-actin (cat# A2228; 1/10,000 (v/v) dilution) was from Sigma-Aldrich; cyclin C (cat# 558903; 1/1000 (v/v) dilution) was from BD Biosciences; CDK8 antibody was obtained from Bethyl (cat# A302-501; 1/1,000 (v/v) dilution); total STAT1 (cat# 14994; 1/1,000 (v/v) dilution), p-STAT1 Tyr701 (cat# 9167; 1/1,000 (v/v) dilution), p-STAT1 Ser727 (cat# 9177; 1/1,000 (v/v) dilution), total IκBα (cat #4814; 1/1,000 (v/v) dilution), pIKKα/β S176/180 (cat# 2697; 1/1,000 (v/v) dilution), total IKKα (cat# 11930; 1/1,000 (v/v) dilution), total c-Jun (cat #9165; 1/1,000 (v/v) dilution), phospho-c-Jun Ser63 (cat# 9261; 1/1,000 (v/v) dilution) and phospho-c-Jun Ser243 (cat# 2994; 1/1000 (v/v) dilution) were from Cell Signaling Technologies.

mRNA isolation

mRNA was isolated from cultured cells using a Dynabeads mRNA DIRECT Kit (Thermo Fisher Scientific) according to the manufacturer's protocol. Briefly, culture media was removed from BMDCs cultured in a 96-well tissue culture treated plate and cells washed with PBS before suspension in lysis buffer. Lysates were incubated with Oligo $(dT)_{25}$ Dynabeads at room temperature for 5 min. Beads were magnetically separated from the lysate and washed 3× with wash buffer A and 1× with wash buffer B before being transferred to a fresh 96-well plate. mRNA was released by suspension of beads in dH_2O and beads removed magnetically. cDNA was prepared from purified mRNA using an iScript cDNA Synthesis kit (Bio-Rad) and diluted 1/10 in dH_2O.

qPCR

Diluted cDNA was quantified by qPCR using the iQ SYBR Green Supermix (Bio-Rad) on a CFX96 real-time system (Bio-Rad). The relative abundance of each mRNA was calculated from Ct values and normalized relative to the abundance of *B2m* mRNA using the $2^{-\Delta\Delta Ct}$ method[47]. The primers used are as follows:

Il10-F, 5′-GCTCTTACTGACTGGCATGAG-3′;

Il10-R, 5′-CGCAGCTCTAGGAGCATGTG-3′;

B2m-F, 5′-TTCTGGTGCTTGTCTCACTGA-3′;

B2m-R, 5′-CAGTATGTTCGGCTTCCCATTC-3′;

Cytokine detection

Release of IL-10 from activated BMDMs and BMDCs or human DCs was quantified using BD ELISA kits (cat #555252 and cat #555157, respectively) according to the manufacturer's protocol. Alternatively, culture medium from stimulated BMDCs was removed and clarified by centrifugation for 5 min at 14,000 × *g*. Levels of TNFα, IL-6, IL-10, or IL-1β in culture medium were quantified using FlexSet Cytokine Bead Array (BD Biosciences) according to the manufacturer's protocol.

Simultaneous signaling pathway activity inference and global gene expression analysis

Preparation of the TF-Seq multiplex reporter library from BMDMs was conducted essentially as described previously[22]. Briefly, BMDMs were differentiated in pen–strep containing DMEM plus 30% FBS and 10% L929 M-CSF conditioned medium (CMG). BMDMs were transduced with an equimolar pool of lentiviral sequencing-based gene reporters (TF-seq) in 90% concentrated lentiviral supernatant + 10% CMG on day 4. On day 7 BMDMs were frozen in 90% FBS and 10% DMSO and stored in liquid nitrogen. BMDMs were thawed in DMEM plus 30% FBS and 10% L929 M-CSF for 2 d before they were harvested from petri dishes (BD Falcon), counted on a hemocytometer, and plated overnight in DMEM + 10% FBS at 100,000 cells/well in 96-well tissue-culture-treated plates (Corning). BMDMs were pretreated with dCA (0.1 μM) or BRD6989 (5 μM) or an equivalent concentration of DMSO (≤0.5%) for 24 h at 37 °C before stimulation with a panel of innate immune ligands (final concentrations: R848 (10 μg/mL); LPS (100 ng/mL) or zymosan A (5 μg/mL). Pam3Cys (300 ng/mL); poly(I:C) (20 μg/mL); CpG (5 μM); FLA

(5 μg/mL); MDP (10 μg/mL); TDB (20 μg/mL); or SeV (10 MOI)) in a short 3-h time series. After defined periods of stimulation, cells were lysed in RLT lysis buffer (Qiagen) and stored at –80 °C. Total RNA was precipitated in 10% PEG 8000 and 1.5 M NaCl, and then washed once in 10% PEG 8000 and 1.5 M NaCl. Purified total RNA was then then resuspended in 50 μL with 2 units TURBO DNase (Life Technologies) and incubated at 37 °C for 30 min. The DNase was denatured by adding 75 μL of RLT lysis buffer and the remaining RNA re-precipitated and washed twice in 10% PEG 8000 and 1.25 M NaCl. Maxima reverse transcriptase (Thermo Scientific) was run according to the manufacturer's instructions using a multiplexed primed reverse transcriptase reaction containing 96-well sequence tagged gene reporter primers, specific to luciferase, and 96-well tagged polydT primers were used at 750 nM and 250 nM final concentrations respectively with 50 units of Maxima. After sequencing tagging all first-strand cDNA during reverse transcriptase, each 96-well plate was pooled and the unincorporated primers were washed away from the cDNA by precipitating with 10% PEG 8000 and 1.25 M NaCl. After RNase A treatment at 37 °C for 30 min, 10% of the first strand cDNA was used in a PCR reaction with Illumina-compatible sequencing primers targeted to the luciferase gene reporter transcripts. The gene reporter amplicon was then sequenced using a 50 cycle PE Illumina Miseq kit. The remaining first-strand cDNA was then converted to double-strand cDNA using the Second Strand Synthesis Module (NEB). 1 ng of the double-strand cDNA (ds-cDNA) libraries was then tagmented with Nextera XT (Illumina) according to the manufacturer's protocol. The pooled cDNA libraries for global gene expression are sequence-tagged only on the 3′ end of the sense transcript, therefore, after full-length ds-cDNA tagmentation we performed enrichment PCR of only the sequence-tagged 3′ end of the mRNA transcript by combining the Nextera N700 series of primers with the Tru-Seq P5 adaptor by means of sequence complementarity introduced during reverse transcriptase priming. This process creates 3′ digital gene expression libraries and was sequenced using 1 flow cell on the Illumina NextSeq machine.

Analysis of gene expression and TF-seq data

For pathway reporter data, we counted the number of unique RNA molecules for every well and reporter, requiring a perfect match for the respective tags. In 3′ gene expression data we first mapped the genomic read to the RefSeq (mm10) transcript sequences using Burrows–Wheeler alignment with default settings[48]. Then we counted the number of unique RNA molecules mapping to each gene in each well, using the RNA UMI and well barcodes embedded into the other read. The resulting count matrices for reporters and genes were analyzed identically using negative binomial generalized linear models from the EdgeR package that are optimized for analyzing count data[49]. We analyzed all of the stimulations individually with a linear model in which we compared the drug effect to DMSO while subtracting the effect of time, using Benjamini–Hochberg FDR < 0.05 as a significance threshold. The set of consistently regulated genes was found by aggregating significant genes from different stimulations using Robust Rank Aggregation algorithm[50]. Significance threshold of 0.05 was applied to Bonferroni corrected aggregation *P* values. To identify enriched Chip-seq binding within this group of genes, we first downloaded the binding scores for multiple transcription factors and chromatin modifications from LPS stimulated BMDMs[23]. First, we associated the binding peaks to the closest gene and then added up all

the scores for all peaks associated to a gene. Based on these scores we ranked all genes and used Wilcoxon test to compare the rankings of our gene set to 1,000 most highly expressed genes in our data set.

Statistical analysis

Results of pilot studies and/or previously completed experiments in similar assay systems were used to estimate sample sizes[9]. Unless otherwise indicated, error bars represent mean ± s.d. for three biological replicates from one independent experiment that is representative of at least two independent experiments. Variance could not be determined for comparisons of small sample sizes. EC_{50}s for IL-10 upregulation and IC_{50}s for CDK8 inhibition were estimated using 4-parameter nonlinear regression in Prism6 (GraphPad). Statistical significance of differences between experimental groups was assessed using unpaired, two-tailed Student *t* test or one-way ANOVA with Dunnett post-test as indicated with Prism6. Unless otherwise indicated, $*P < 0.05$; $**P < 0.01$; $***P < 0.001$.

Data availability

All data generated or analyzed during this study are included in this published article (and its Supplementary Information files) or are available from the corresponding author on reasonable request. Primary RNA-seq data used to generate Supplementary Figure 8b are available from the NIH Gene Expression Omnibus (accession number GSE99759).

Supplementary Material

Refer to Web version on PubMed Central for supplementary material.

Acknowledgments

This work was supported by funding from the National Institutes of Health Grants K08DK104021 (B.K.), R01CA190509 (P.S.), U01DK062432 and P30DK043351 (R.J.X.); Crohn's and Colitis Foundation of America Grant 500229 (R.J.X.); and The Leona M. and Harry B. Helmsley Charitable Trust Grant 500203 (S.L.S. and R.J.X.). S.L.S. is an Investigator of the Howard Hughes Medical Institute. We thank P. Baran (The Scripps Research Institute) for the generous gift of Δ^{16}-cortistatin A.

References

1. Saraiva M, O'Garra A. The regulation of IL-10 production by immune cells. Nat Rev Immunol. 2010; 10:170–181. [PubMed: 20154735]
2. Shouval DS, et al. Interleukin 10 receptor signaling: master regulator of intestinal mucosal homeostasis in mice and humans. Adv Immunol. 2014; 122:177–210. [PubMed: 24507158]
3. Asadullah K, Sterry W, Volk HD. Interleukin-10 therapy–review of a new approach. Pharmacol Rev. 2003; 55:241–269. [PubMed: 12773629]
4. Braat H, et al. A phase I trial with transgenic bacteria expressing interleukin-10 in Crohn's disease. Clin Gastroenterol Hepatol. 2006; 4:754–759. [PubMed: 16716759]
5. Galeazzi M, et al. A phase IB clinical trial with Dekavil (F8-IL10), an immunoregulatory 'armed antibody' for the treatment of rheumatoid arthritis, used in combination wiIh methotrexate. Isr Med Assoc J. 2014; 16:666. [PubMed: 25438467]
6. Rodríguez M, et al. Polarization of the innate immune response by prostaglandin E2: a puzzle of receptors and signals. Mol Pharmacol. 2014; 85:187–197. [PubMed: 24170779]

7. Martin M, Rehani K, Jope RS, Michalek SM. Toll-like receptor-mediated cytokine production is differentially regulated by glycogen synthase kinase 3. Nat Immunol. 2005; 6:777–784. [PubMed: 16007092]
8. Clark K, et al. Phosphorylation of CRTC3 by the salt-inducible kinases controls the interconversion of classically activated and regulatory macrophages. Proc Natl Acad Sci USA. 2012; 109:16986–16991. [PubMed: 23033494]
9. Sundberg TB, et al. Small-molecule screening identifies inhibition of salt-inducible kinases as a therapeutic strategy to enhance immunoregulatory functions of dendritic cells. Proc Natl Acad Sci USA. 2014; 111:12468–12473. [PubMed: 25114223]
10. Wang B, et al. Microtubule acetylation amplifies p38 kinase signalling and anti-inflammatory IL-10 production. Nat Commun. 2014; 5:3479. [PubMed: 24632940]
11. Na YR, et al. The early synthesis of p35 and activation of CDK5 in LPS-stimulated macrophages suppresses interleukin-10 production. Sci Signal. 2015; 8:ra121. [PubMed: 26602020]
12. Souto A, Gómez-Reino JJ. Apremilast for the treatment of psoriatic arthritis. Expert Rev Clin Immunol. 2015; 11:1281–1290. [PubMed: 26503917]
13. Gordon JN, et al. CC-10004 but not thalidomide or lenalidomide inhibits lamina propria mononuclear cell TNF-α and MMP-3 production in patients with inflammatory bowel disease. J Crohns Colitis. 2009; 3:175–182. [PubMed: 21172267]
14. Xing L, Rai B, Lunney EA. Scaffold mining of kinase hinge binders in crystal structure database. J Comput Aided Mol Des. 2014; 28:13–23. [PubMed: 24375079]
15. Allen BL, Taatjes DJ. The Mediator complex: a central integrator of transcription. Nat Rev Mol Cell Biol. 2015; 16:155–166. [PubMed: 25693131]
16. Bancerek J, et al. CDK8 kinase phosphorylates transcription factor STAT1 to selectively regulate the interferon response. Immunity. 2013; 38:250–262. [PubMed: 23352233]
17. Shi J, et al. Scalable synthesis of cortistatin A and related structures. J Am Chem Soc. 2011; 133:8014–8027. [PubMed: 21539314]
18. Pelish HE, et al. Mediator kinase inhibition further activates super-enhancer-associated genes in AML. Nature. 2015; 526:273–276. [PubMed: 26416749]
19. Mallinger A, et al. Discovery of potent, selective, and orally bioavailable small-molecule modulators of the mediator complex-associated kinases CDK8 and CDK19. J Med Chem. 2016; 59:1078–1101. [PubMed: 26796641]
20. Kwiatkowski N, et al. Targeting transcription regulation in cancer with a covalent CDK7 inhibitor. Nature. 2014; 511:616–620. [PubMed: 25043025]
21. Li N, et al. Cyclin C is a haploinsufficient tumour suppressor. Nat Cell Biol. 2014; 16:1080–1091. [PubMed: 25344755]
22. O'Connell DJ, et al. Simultaneous pathway activity inference and gene expression analysis using RNA sequencing. Cell Syst. 2016; 2:323–334. [PubMed: 27211859]
23. Garber M, et al. A high-throughput chromatin immunoprecipitation approach reveals principles of dynamic gene regulation in mammals. Mol Cell. 2012; 47:810–822. [PubMed: 22940246]
24. Witte S, O'Shea JJ, Vahedi G. Super-enhancers: Asset management in immune cell genomes. Trends Immunol. 2015; 36:519–526. [PubMed: 26277449]
25. Shlyueva D, Stampfel G, Stark A. Transcriptional enhancers: from properties to genome-wide predictions. Nat Rev Genet. 2014; 15:272–286. [PubMed: 24614317]
26. Porter DC, et al. Cyclin-dependent kinase 8 mediates chemotherapy-induced tumor-promoting paracrine activities. Proc Natl Acad Sci USA. 2012; 109:13799–13804. [PubMed: 22869755]
27. Poss ZC, et al. Identification of mediator kinase substrates in human cells using cortistatin A and quantitative phosphoproteomics. Cell Reports. 2016; 15:436–450. [PubMed: 27050516]
28. Yamamoto S, et al. Mediator cyclin-dependent kinases upregulate transcription of inflammatory genes in cooperation with NF-κB and C/EBPβ on stimulation of Toll-like receptor 9. Genes Cells. 2017; 22:265–276. [PubMed: 28151579]
29. Lin A, et al. Casein kinase II is a negative regulator of c-Jun DNA binding and AP-1 activity. Cell. 1992; 70:777–789. [PubMed: 1516134]

30. Huang CC, et al. Calcineurin-mediated dephosphorylation of c-Jun Ser-243 is required for c-Jun protein stability and cell transformation. Oncogene. 2008; 27:2422–2429. [PubMed: 17952113]
31. Taira N, et al. DYRK2 priming phosphorylation of c-Jun and c-Myc modulates cell cycle progression in human cancer cells. J Clin Invest. 2012; 122:859–872. [PubMed: 22307329]
32. Aikawa Y, et al. Treatment of arthritis with a selective inhibitor of c-Fos/activator protein-1. Nat Biotechnol. 2008; 26:817–823. [PubMed: 18587386]
33. Lim S, Kaldis P. Cdks, cyclins and CKIs: roles beyond cell cycle regulation. Development. 2013; 140:3079–3093. [PubMed: 23861057]
34. Saraiva M, et al. Identification of a macrophage-specific chromatin signature in the IL-10 locus. J Immunol. 2005; 175:1041–1046. [PubMed: 16002704]
35. Donner AJ, Ebmeier CC, Taatjes DJ, Espinosa JM. CDK8 is a positive regulator of transcriptional elongation within the serum response network. Nat Struct Mol Biol. 2010; 17:194–201. [PubMed: 20098423]
36. Schreiber S, et al. Safety and efficacy of recombinant human interleukin 10 in chronic active Crohn's disease. Crohn's disease IL-10 cooperative study group. Gastroenterology. 2000; 119:1461–1472. [PubMed: 11113067]
37. Marlow GJ, van Gent D, Ferguson LR. Why interleukin-10 supplementation does not work in Crohn's disease patients. World J Gastroenterol. 2013; 19:3931–3941. [PubMed: 23840137]
38. Itakura E, et al. IL-10 expression by primary tumor cells correlates with melanoma progression from radial to vertical growth phase and development of metastatic competence. Mod Pathol. 2011; 24:801–809. [PubMed: 21317876]
39. Pyonteck SM, et al. CSF-1R inhibition alters macrophage polarization and blocks glioma progression. Nat Med. 2013; 19:1264–1272. [PubMed: 24056773]
40. Wang S, et al. Expression of CD163, interleukin-10, and interferon-gamma in oral squamous cell carcinoma: mutual relationships and prognostic implications. Eur J Oral Sci. 2014; 122:202–209. [PubMed: 24796206]
41. Clarke PA, et al. Assessing the mechanism and therapeutic potential of modulators of the human Mediator complex-associated protein kinases. eLife. 2016; 5:e20722. [PubMed: 27935476]
42. Yamaoka K. Janus kinase inhibitors for rheumatoid arthritis. Curr Opin Chem Biol. 2016; 32:29–33. [PubMed: 26994322]
43. Miller SC, et al. Identification of known drugs that act as inhibitors of NF-kappaB signaling and their mechanism of action. Biochem Pharmacol. 2010; 79:1272–1280. [PubMed: 20067776]
44. Sundberg TB, et al. Development of chemical probes for investigation of salt-inducible kinase function *in vivo*. ACS Chem Biol. 2016; 11:2105–2111. [PubMed: 27224444]
45. Wawer MJ, et al. Toward performance-diverse small-molecule libraries for cell-based phenotypic screening using multiplexed high-dimensional profiling. Proc Natl Acad Sci USA. 2014; 111:10911–10916. [PubMed: 25024206]
46. Duan Q, et al. LINCS Canvas Browser: interactive web app to query, browse and interrogate LINCS L1000 gene expression signatures. Nucleic Acids Res. 2014; 42:W449–W460. [PubMed: 24906883]
47. Pfaffl MW. A new mathematical model for relative quantification in real-time RT-PCR. Nucleic Acids Res. 2001; 29:e45. [PubMed: 11328886]
48. Li H, Durbin R. Fast and accurate short read alignment with Burrows-Wheeler transform. Bioinformatics. 2009; 25:1754–1760. [PubMed: 19451168]
49. Robinson MD, McCarthy DJ, Smyth GK. edgeR: a Bioconductor package for differential expression analysis of digital gene expression data. Bioinformatics. 2010; 26:139–140. [PubMed: 19910308]
50. Kolde R, Laur S, Adler P, Vilo J. Robust rank aggregation for gene list integration and meta-analysis. Bioinformatics. 2012; 28:573–580. [PubMed: 22247279]

Editorial Summary

Inhibitors of CDK8 enhance IL-10 production during innate immune activation in human and mouse primary macrophages and dendritic cells via diminished phosphorylation of the c-Jun subunit of the AP-1 transcription regulation complex.

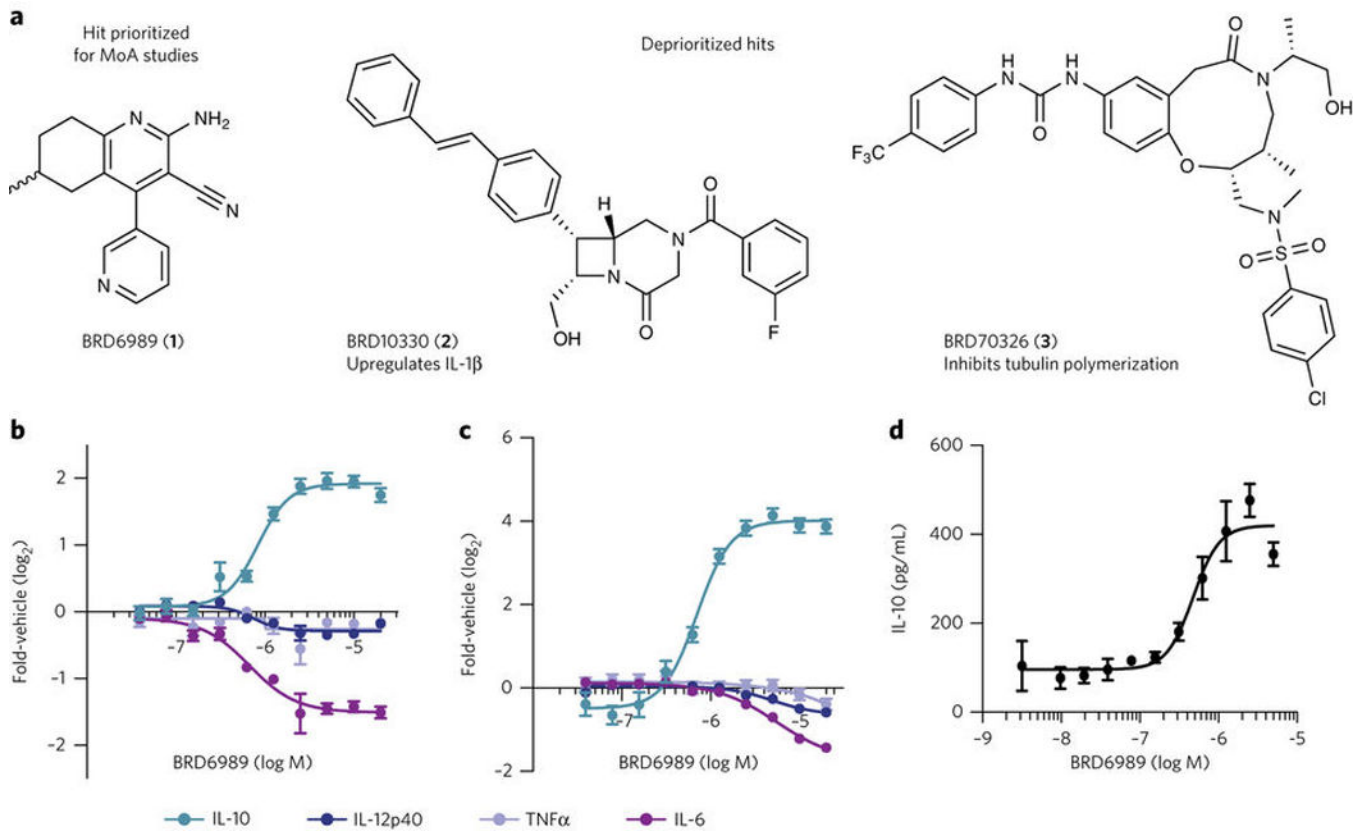

Figure 1. BRD6989 prioritized from phenotypic screen for small-molecule enhancers of IL-10 production

(**a**) Chemical structures of BRD6989 (**1**) and the deprioritized screening hits BRD10330 (**2**) and BRD70326 (**3**) with the rationale for their deprioritization. (**b**,**c**) Effect of BRD6989 on cytokine production in BMDCs stimulated with zymosan A (**b**) or R848 (**c**). Each point corresponds to mean ± s.d.; $n = 3$ biological replicates from one independent experiment; Data represent three independent experiments. Vehicle corresponds to DMSO (≤0.5%). (**d**) Effect of BRD6989 on IL-10 production in human DCs stimulated with R848. Each point corresponds to mean ± s.d.; $n = 3$ biological replicates from one independent experiment using cells derived from one donor; Data represent two independent experiments (see Supplementary Fig. 3).

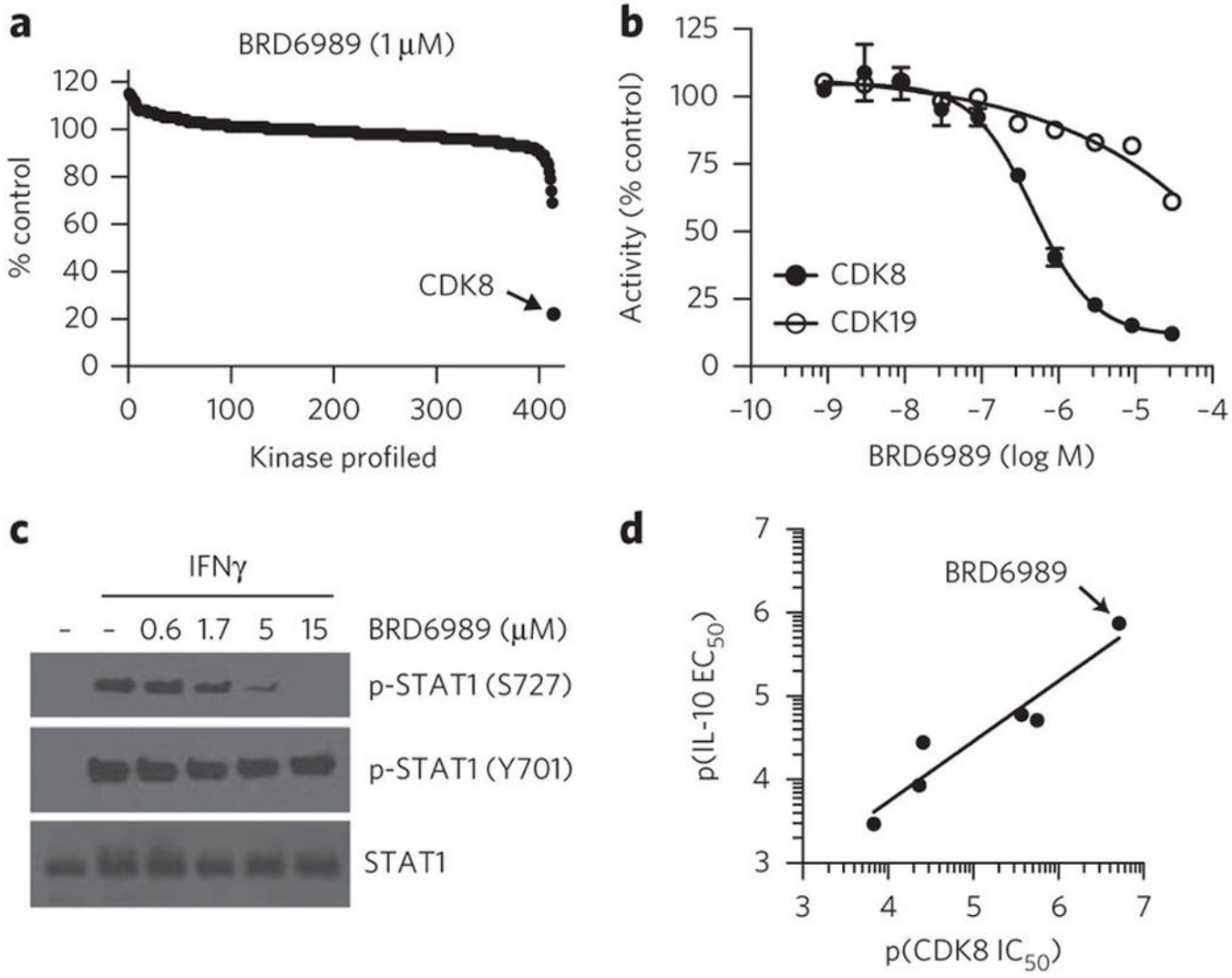

Figure 2. CDK8 is a molecular target of BRD6989

(**a**) Kinase profiling identifies cyclin C–CDK8 as a molecular target of BRD6989. Each point corresponds to the mean of three biological replicates from one independent experiment normalized to a DMSO (≤0.5%) control (see Supplementary Data Set 1). (**b**) Effect of the indicated concentrations of BRD6989 on the activity of cyclin C–CDK8 or cyclin C–CDK19 complexes. Each point corresponds to mean ± s.d.; $n = 3$ biological replicates from one independent experiment for cyclin C–CDK8 or $n = 2$ biological replicates from one independent experiment for cyclin C–CDK19 normalized to a DMSO (1%) control. (**c**) BRD6989 suppresses phosphorylation of the STAT1 transactivation domain at Ser727 in IFNγ-stimulated BMDCs. Data represent three independent experiments; full gel images are presented in Supplementary Figure 11. (**d**) CDK8 binding affinity correlates with the potency of IL-10 upregulation for BRD6989 and its derivatives. $R^2 = 0.91$ for linear regression; IC_{50} and EC_{50} data are from one independent experiment and have been transformed to a negative $\log_{10}$ (p) scale (see Supplementary Fig. 5).

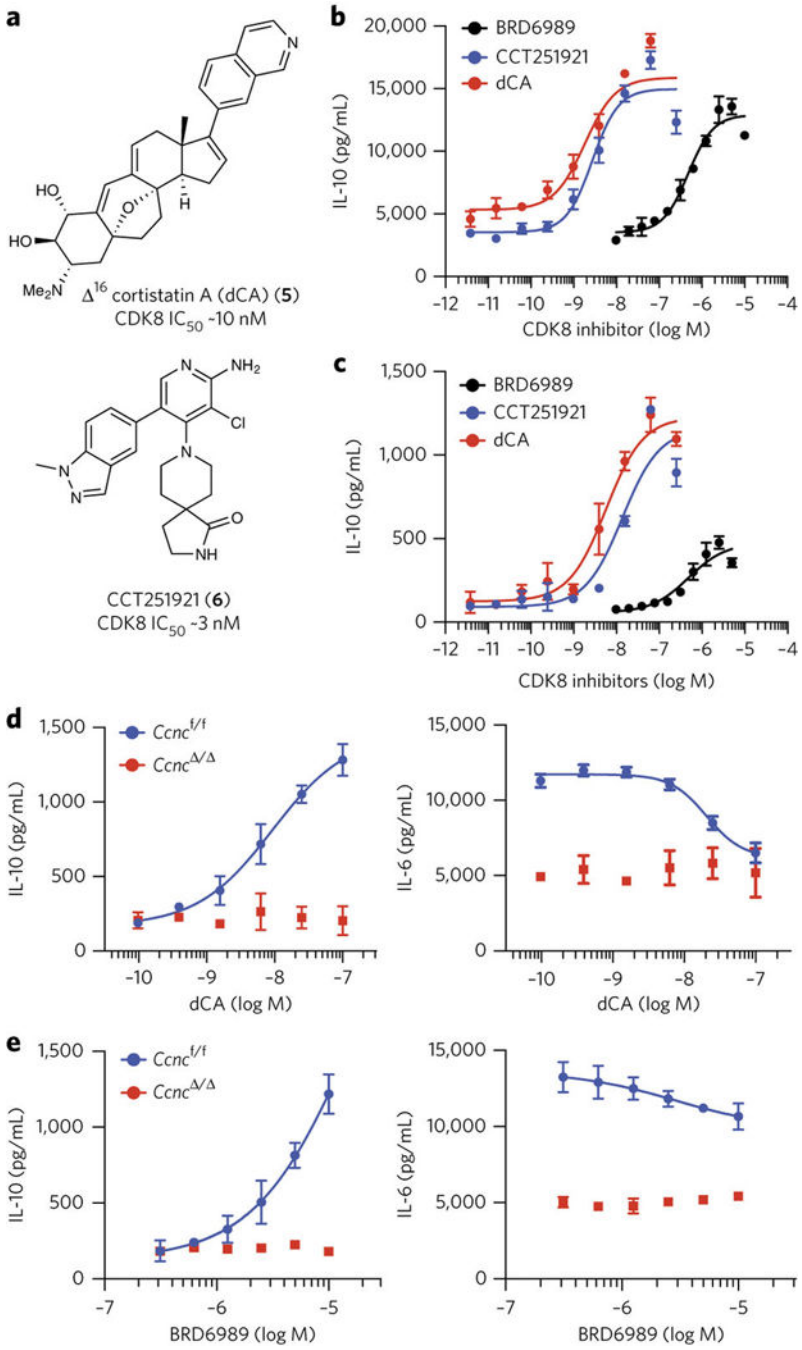

Figure 3. Pharmacological and genetic data identify CDK8 as a negative regulator of IL-10 production

(**a**) Chemical structures of the potent, specific CDK8 and CDK19 inhibitors Δ^{16}-cortistatin A (dCA; **5**) and CCT251921 (**6**). (**b**) CCT251921 and dCA recapitulate the IL-10-enhancing activity of BRD6989 in R848-stimulated BMDCs. Each point corresponds to mean ± s.d.; *n* = 3 biological replicates from one independent experiment; data represent three independent experiments. (**c**) CCT251921 and dCA recapitulate IL-10 potentiation by BRD6989 in human DCs stimulated with R848. Each point corresponds to mean ± s.d.; *n* = 3 biological

replicates from one independent experiment using cells derived from one donor; data represent two independent experiments (see Supplementary Fig. 6). (**d**,**e**) Deletion of cyclin C in BMDCs derived from *Ccnc*$^{\Delta/\Delta}$ mice impairs induction of IL-10 and suppression of IL-6 by dCA (**d**) or BRD6989 (**e**) following activation with R848. Each point corresponds to mean ± s.d.; $n = 4$ biological replicates from one independent pair of *Ccnc*$^{\Delta/\Delta}$ or *Ccnc*$^{f/f}$ mice; data represent three independent experiments (see Supplementary Fig. 7).

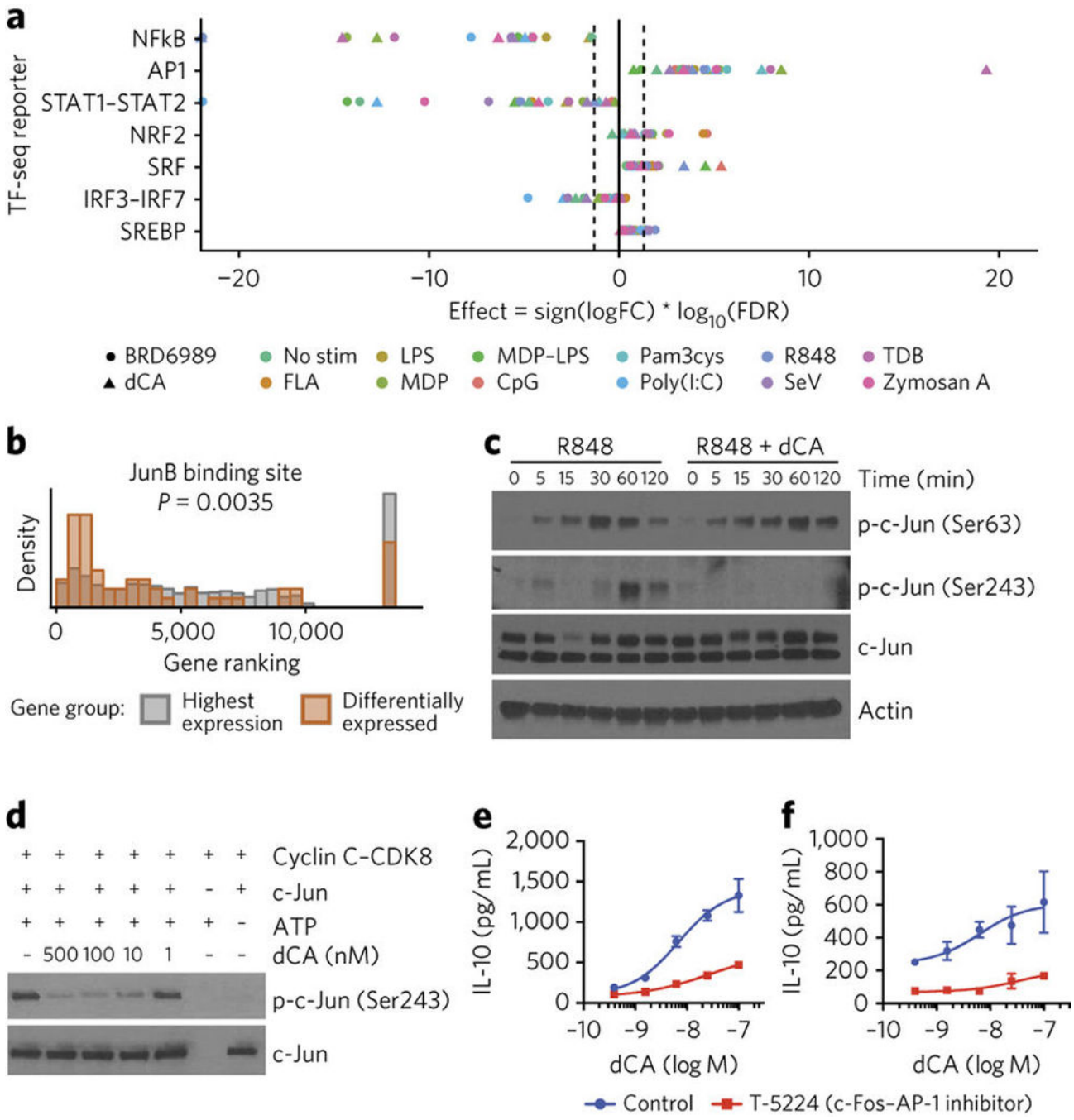

Figure 4. Modulation of c-Jun–AP-1 links CDK8 inhibition to enhanced IL-10 production

(**a**) CDK8-responsive signaling pathways in activated BMDMs as identified by the highly parallel reporter gene assay TF-seq. Reporter data are integrated for time points between 0.25 and 4 h from one independent experiment (See Online Methods and Supplementary Data Set 4). Dashed lines correspond to false discovery rate (FDR) < 0.05 as corrected by Benjamini–Hochberg testing. no stim, no stimulation; FLA, flagellin A; LPS, lipopolysaccharide; MDP, muramyldipeptide; CpG, synthetic CpG-containing oligonucleotide; Pam3cys, synthetic triacylated lipoprotein; poly(I:C), polyinosinic–

polycytidylic acid; SeV, Sendai virus; TDB, trehalose-6,6-dibehenate. (**b**) In comparison to all highly expressed genes, JunB binding sites are enriched among the subset of genes induced by CDK8 inhibition (see Online Methods). (**c**) Pretreatment with dCA (100 nM; 18 h) suppresses phosphorylation (p) of c-Jun on Ser243 in BMDCs activated with R848 for the indicated times. Data represent two independent experiments; full images are presented in Supplementary Figure 12. (**d**) The indicated concentrations of dCA suppress phosphorylation of recombinant c-Jun at Ser243 by recombinant cyclin C–CDK8 in an *in vitro* kinase reaction. Data represent two independent experiments; full images are presented in Supplementary Figure 12. (**e**,**f**) Co-treatment of BMDCs with the c-Fos–AP-1 inhibitor T-5224 (100 μM) suppresses the IL-10 enhancing activity of dCA in BMDCs stimulated with R848 (**e**) or zymosan A (**f**) relative to DMSO (≤0.5%) control. Each point correspond to mean ± s.d.; $n = 3$ biological replicates from one independent experiment; data represent three independent experiments.